Chapter 4

Silver Nanoparticles Entangled Polythiophene-Functionalized MWCNT Ternary Nanocomposites: A Green Synthetic Approach and Enhancement in Properties

4.1. Introduction

The preparation of higher-order structural architectures from binary nanocomposites would be advantageous for their better performance or for exploring more areas of application.[1-3] Functionalized multiwalled carbon nanotube nanocomposites with conducting polymer via the formation of core-shell morphology can act as an effective synergistic host to accommodate different materials. A sizeable surface-to-volume ratio in nanostructured conducting polythiophene-CNT nanocomposites would be beneficial to incorporate additional nanofillers to the surface of its lightweight framework.[4,5]

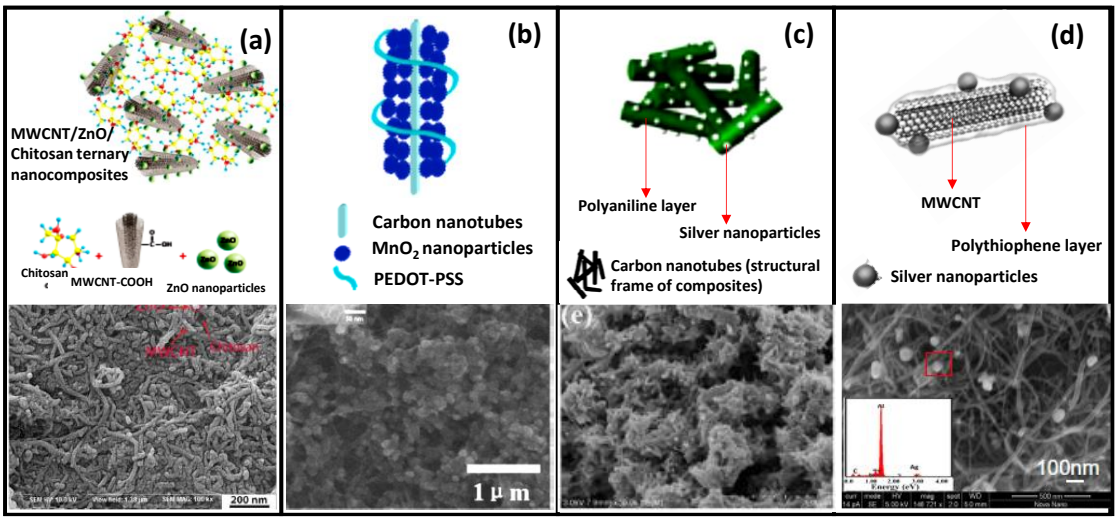

Figure 4.1. *Metal nanoparticles incorporation with different polymer-carbon nanotube nanocomposites and their scanning electron microscopic images (adapted from (a) malekkiani et al. 2022 (b) Hou et al. 2010 (c) Tang et al. 2016 and (d) Patole et al. 2015.)*

Incorporating metal nanoparticles as fillers into conducting polymer-carbon nanotube nanocomposites find new applications by gaining additional properties with enhanced performance. Structurally different morphologies can be obtained for such ternary nanocomposites based on synthetic routes, types of polymer, and the nature of the incorporated metal. Some of the reports of ternary systems of polymer-carbon nanotube nanocomposites with metal nanoparticles are shown in **figure 4.1.**[6-9] Silver nanoparticles are an attractive choice among metal fillers as it exhibits high electrical and thermal conductivity.[10] Distinct characteristics of silver nanoparticles rendering different applications such as catalysis, surface-plasmon resonance, antimicrobial

action, surface-enhanced Raman scattering tags, therapeutic usages, electrochemical applications, electromagnetic interference (EMI) shielding etc.[11-13] However, the long-term use of bare silver nanoparticles as such is not viable due to the high surface charges on nanoparticles, which create low negative fermi potential and get aggregated easily.[14] Stable silver nanoparticles require suitable capping agents to avoid their tendency of aggregation.[12] Inorganic or polymeric stabilizing supports can be effectively used against aggregation and promote the silver nanoparticle's stability.[14,15]

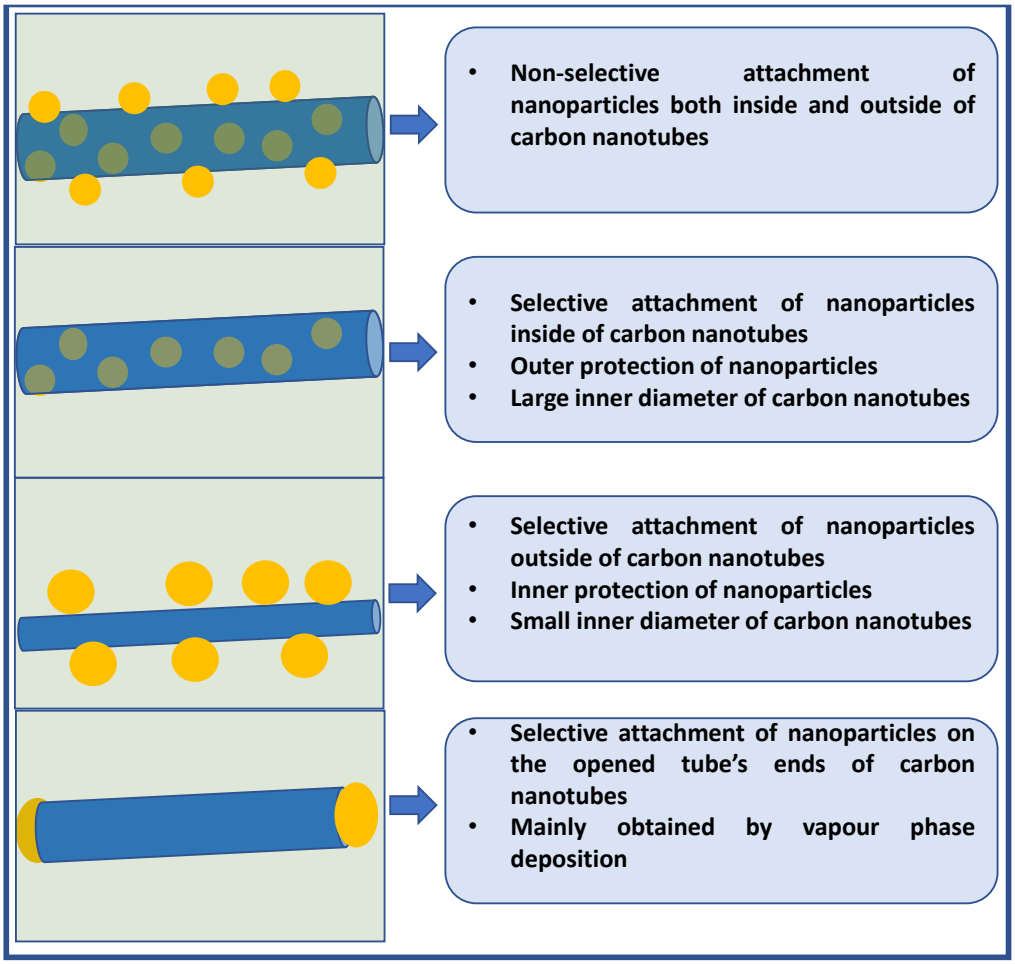

Figure 4.2. *Different possibilities for the formation of carbon nanotube-metal nanoparticle nanocomposites.*

The incorporation of silver nanoparticles with polymer materials can generally be carried out in two different ways. One method is the *in-situ* synthesis of silver nanoparticles in the presence of a polymer scaffold. The second method is the *ex-situ* attachment of silver nanoparticles to the desired polymer material.[15,16] Preparation of silver nanoparticles with polymerization in a single step is also reported rarely.[17] An

advantage of *in-situ* preparation is the uniform attachment of soluble silver ions with the pre-structured polymer framework, producing a homogeneous distribution of nanoparticles with the solid matrix.[15] Selection of suitable polymer material should also required for excellent properties. Conducting polythiophene exhibits good environmental stability and compatibility with silver nanoparticles.[18] Polymer alone or in hybrid/composite form could be used as a suitable scaffold to accommodate silver nanoparticles. The structural features of scaffolding materials are essential to control the size, shape and assembly of metal nanoparticles formed.[19,20] Among different scaffolding materials to accommodate in-situ formed silver nanoparticles, core-shell structured polythiophene-carbon nanotube binary nanocomposites would be attractive for its typical characteristics such as one-dimensional nano-structural confinement, conducting host framework, good thermal stability and ability to form a stable aqueous dispersion. Methods of area specific and area non-specific attachment of metal nanoparticles in carbon nanotubes are schematically represented in **Figure 4.2.** The selective area attachment of nanoparticles on inner walls, outer walls and/or end caps are possible, and they possess unique benefits leading to specific applications.[21-25]

Adopting green approaches for silver nanoparticles embedded polythiophene-functionalized multiwalled carbon nanotube ternary nanocomposites can render several benefits, such as cost-effectiveness, good dispersibility in the aqueous phase, high electrical conductivity, and thermal stability.[26,27] Applications of prepared silver nanocomposites will be determined by their processability and other properties.[28] Studies on ternary nanocomposites incorporating stable silver nanoparticles into polythiophene-functionalized multiwalled carbon nanotubes were rarely reported. Patole et al. reported the preparation of PEDOT/PSS-ethylenediamine functionalized multiwalled carbon nanotube-silver nanoparticle nanocomposites by reduction of $AgNO_3$ using $NaBH_4$ in dichloromethane medium for improving electrical conductivity and thermal properties of polycarbonate matrix. Studies on the bicomponent systems, such as polythiophene-silver nanocomposites or carbon nanotube-silver nanocomposites, were conducted by various researchers. A recent literature review by Al-Refai et. al. based on polythiophene nanocomposites discusses the advantages and relevance of incorporating nanomaterials such as metal nanoparticles and carbon nanotubes into polythiophene matrix.[28] The ternary structural combination of silver

nanoparticles into a polythiophene-carbon nanotube nanocomposite framework could open up various applications with cohesive properties.

In the present chapter, we have put forward a facile and green synthetic approach for developing silver nanoparticles embedded in polythiophene-functionalized multiwalled carbon nanotube nanocomposites by reduction of silver nitrate using ascorbic acid (Vitamin-C) in an aqueous medium. Binary nanocomposite (PTCNT-COOH 300) acted as a nanofibrous template in which silver nanoparticles grew to form a ternary nanocomposite. Here, the polythiophene-functionalized multiwalled carbon nanotube nanocomposites act as a stable framework to accommodate and protect highly labile silver atoms as solid nanoparticles; otherwise, it might agglomerate in the absence of a strong capping agent. Interestingly, the tangled silver nanoparticles embedded ternary polythiophene-functionalized MWCNT nanocomposites having good dispersibility in water, high electrical conductivity, good solid-state ordering, and high thermal stability were established.

4.2. Experimental

4.2.1. Materials and reagents used: Silver nitrate and multiwalled carbon nanotubes (MWCNT) were purchased from Sigma Aldrich. Ascorbic acid, sodium hydroxide, hydrochloric acid, acetic acid, ammonium hydroxide, acetone and deionized water were purchased from Merck chemicals India.

4.2.2. Measurements and instruments: Fourier transform-infrared spectra of the samples were recorded by Shimadzu IR Affinity 1 spectrometer using the KBr pellet method. Raman spectra of samples were taken by LabRam spectrometer by HORIBA JOBIN YVON using argon ion laser of wavelength 514.5 nm. UV-vis spectra of the samples were recorded by Shimadzu UV-Visible spectrophotometer, UV 1800 series in the range 200-800 nm with HPLC grade chloroform, ethanol and deionized water. The powder wide-angle X-ray diffraction of the samples was measured using PANALYTICAL, Aeris research with 2θ values ranging from 5 to 80°. The field emission scanning electron microscope (FE-SEM) images were recorded by ZEISS ΣIGMA^{TM} field emission scanning electron microscope. The transmission electron microscopic analysis was carried out by JEOL/JEM 2100 instrument having a capacity of 200 KV and with magnification 2000X – 1500000X. Thermogravimetric analysis (TGA) of the samples was measured using Perkin Elmer, Diamond TG/DTA in an inert

atmosphere of nitrogen at a heating rate of 20°C. The four-probe electrical conductivity of the samples was measured using DFP-RM-200 with constant current source Model CCS-01 and DC microvoltmeter. The pH measurements were carried out using HM digital PH -80 Temp hydro tester. The XPS analysis was carried out using PHI 5000 Versa Probe III instrument. Both wide scan spectra (in the range of 150-600 eV) and narrow scan spectra of individual elements were carried out with XPS spectra.

4.2.3. Synthesis of PTCNT-COOH 300 Ag: The sample PTCNT-COOH 300 (0.16 g) was dispersed in 500 mL of deionized water by sonication. Ascorbic acid (8.81 g, 5.00 mmol) was added to the above binary composite, followed by the addition of NaOH solution (10 M, 20 mL, 21.00 mmol) with magnetic stirring for 5 min and allowed to equilibrate the pH for 3 h. Fresh $AgNO_3$ solution (5 mL, 0.30 M, 1.50 mmol) was added to this mixture under strong stirring conditions for 30 s, followed by gentle stirring for 30 min at room temperature. The mixture was kept undisturbed for 12 h and then washed with deionized water (till the pH of the filtrate became neutral from alkaline). The ternary nanocomposite mixture was finally washed with acetone and dried in a vacuum oven at 70^{o} C. Yield: 0.28 g. FT-IR (KBr, cm^{-1}) 693, 787, 1534, 1646, 1695, and 1747.

4.2.4. Synthesis of MWCNT-COOH Ag: MWCNT-COOH (0.16 g) was dispersed in 500 mL of deionized water by sonication. Ascorbic acid (8.81g, 5.00 mmol) was added to the above dispersion followed by the addition of NaOH solution (10 M, 20 mL, 21.00 mmol) with magnetic stirring for 5 min and allowed to equilibrate the pH for 3 h. Fresh $AgNO_3$ solution (5 mL, 0.30 M, 1.50 mmol) was then added to this mixture under strong stirring conditions for 30 s followed by gentle stirring for 30 min at room temperature. The mixture was kept undisturbed for 12 h and then washed with deionized water (till the pH of the filtrate became neutral from alkaline). The binary silver nanocomposite mixture was finally washed with acetone and dried in a vacuum oven at 70^{o}C. Yield: 0.31 g. FT-IR (KBr, cm^{-1}) 1550, 1646, 1705, 1754.

4.2.5. Leaching study of PTCNT-COOH 300 Ag with different pH: PTCNT-COOH 300 Ag (0.010 g) was dispersed in HCl (15 mL, 1M, pH: 0.8) by sonication for 5 min. Then it was magnetically stirred for 3 h. It was washed with water, filtered and the residue obtained was dried in a vacuum oven at 60°C for 1 h. The above residue was subjected to record UV-Vis spectra by dispersing in water.

The above procedure was repeated by changing the medium into CH_3COOH (1M, pH:2.8), water (pH:7.0), NH_4OH (1M, pH:11.5) and NaOH (1M, pH:12.8).

4.3. Results and Discussion

4.3.1 Synthesis and characterization of PTCNT-COOH 300 Ag and MWCNT-COOH Ag

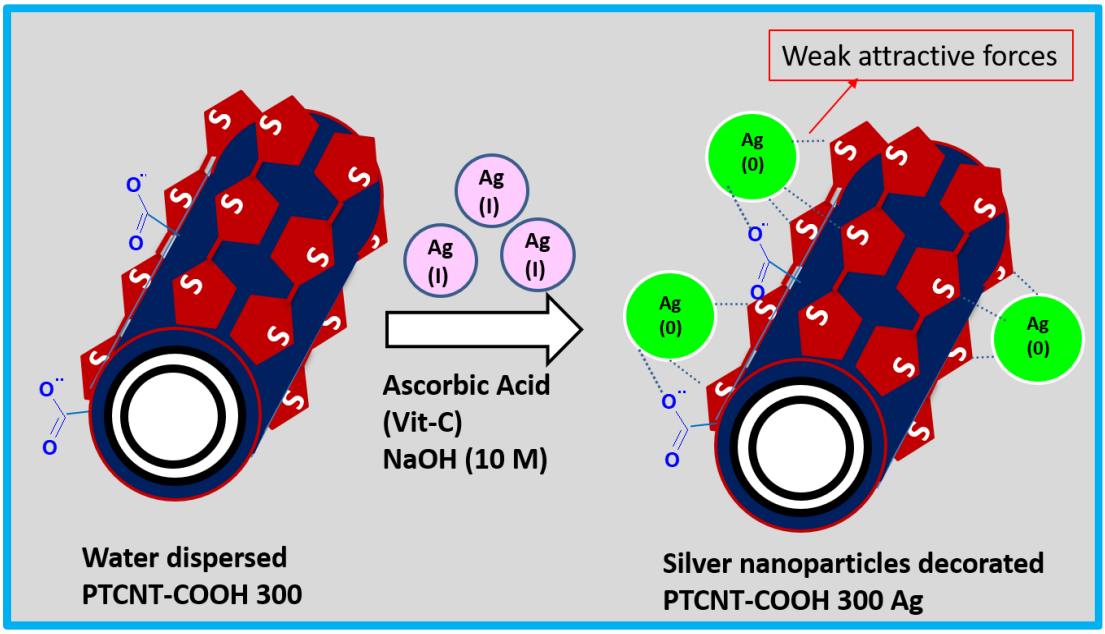

Figure 4.3. *Schematic representation of the synthesis of PTCNT-COOH 300 Ag*

The ternary silver nanocomposite PTCNT-COOH 300 Ag was prepared by reducing silver nitrate solution to silver nanoparticles using ascorbic acid as the reducing agent in the presence of aqueous dispersed PTCNT-COOH 300 nanocomposites. The formation of PTCNT-COOH 300 Ag is schematically represented in **Figure 4.3.** (see **Table 4.1.** also) Ascorbic acid (vitamin C) is a green and bio-friendly reducing reagent. Silver nitrate reduction was carried out in the presence of stable aqueous dispersion of PTCNT-COOH composites discussed in chapter 3. Sonication for 15 min produced stable dispersion of binary PTCNT-COOH 300 nanocomposites. Here, the PTCNT-COOH 300 functioned as a hard template to accommodate the reduced form of silver nanoparticles by providing a large enough surface area in its nanotubular assembly. The synthesis was carried out in basic pH≈10. Control on pH was carried out by adding NaOH solution. The same procedure was also used to synthesize binary silver nanocomposites named MWCNT-COOH Ag formed

by reduction of silver nitrate in presence of functionalized MWCNT-COOH (conducting polythiophene is not present).

Table 4.1. *Atomic concentration of samples from XPS spectra, pH of the samples, morphology of samples, thermal stability of samples, and electrical conductivity of samples.*

Samples	**Components**	**Type of Nano composites**	**Atomic Concentration from XPS (%)**				**pH**	**Shape**	**Thermal Stability (°C)**	**Conductivity (S/cm)**
			C 1s	**O 2s**	**S 2p**	**Ag 3d**				
MWCNT-COOH	-	-	94.42	5.58	-	-	4.8	nanotubes	560	2.80
PTCNT-COOH-300	Thiophene + MWCNT-COOH	Binary	88.63	5.70	5.68	-	5.4	PT covered Nanotubes	340	1.64
MWCNT-COOH Ag	MWCNT-COOH + Ag	Binary	-	-	-	-		Nanoparticles + nanotubes	750	12.40
PTCNT-COOH 300 Ag	Thiophene + Ag + MWCNT-COOH	Ternary	86.66	7.75	4.22	2.37	7.0	Nanoparticles + PT covered Nanotubes	620	80.76

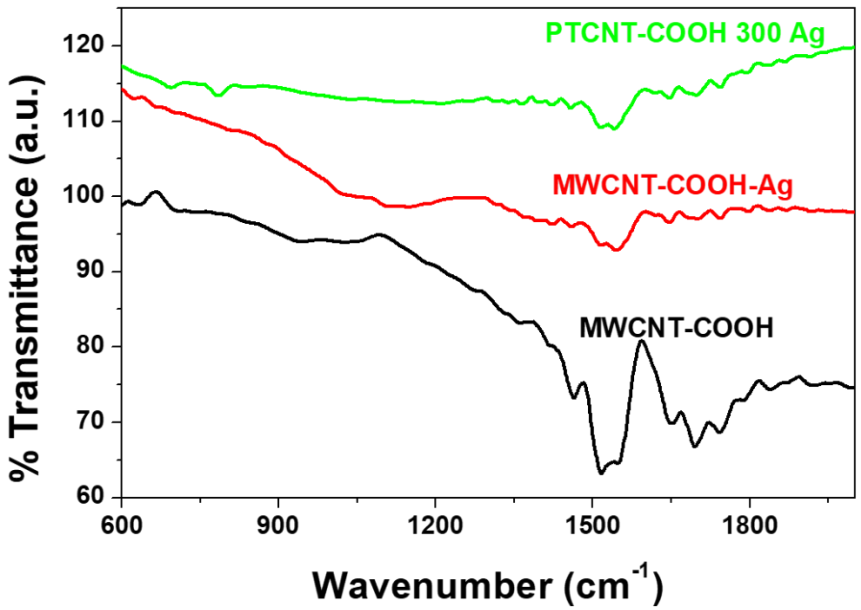

Figure 4.4. *FT-IR spectra of MWCNT-COOH, MWCNT-COOH Ag and PTCNT-COOH 300 Ag*.

PTCNT-COOH 300 Ag and MWCNT-COOH Ag were subjected to FT-IR studies to characterize the formation of respective nanocomposites (see **Figure 4.4.**). The functionalized MWCNT-COOH Ag have shown peaks of MWCNT-COOH at 1534 cm^{-1}, 1646 cm^{-1}, 1695 cm^{-1} and 1747 cm^{-1} corresponding to in-plane vibrations of graphitic walls, C=C stretching vibrations, carbonyl groups and C=O stretching vibration in acid groups respectively. PTCNT-COOH 300 Ag sample has shown characteristic peaks of thiophene at 787 cm^{-1} and 693 cm^{-1} due to C-H out-of-plane deformation mode and C-S stretching mode of the thiophene ring in addition to the peaks of MWCNT-COOH. MWCNT-COOH Ag and PTCNT-COOH 300 Ag samples have shown a decline in carbonyl stretching frequency at 1695 and 1747 cm^{-1}, which could be attributed to the nanocomposites formation with silver. [29-32] FT-Raman spectra of PTCNT-COOH 300 Ag and MWCNT-COOH Ag in powder form were recorded using 514.5 nm argon laser (see **Figure 4.5.**). MWCNT-COOH Ag has shown characteristic G band and D band at 1576 cm^{-1} and 1348 cm^{-1}, respectively. In the case of PTCNT-COOH 300 Ag, an additional intense peak was observed at 1450 cm^{-1} due to symmetric in-phase vibration of the polythiophene chain, which showed the presence of polythiophene in the ternary nanocomposite.[32,33]

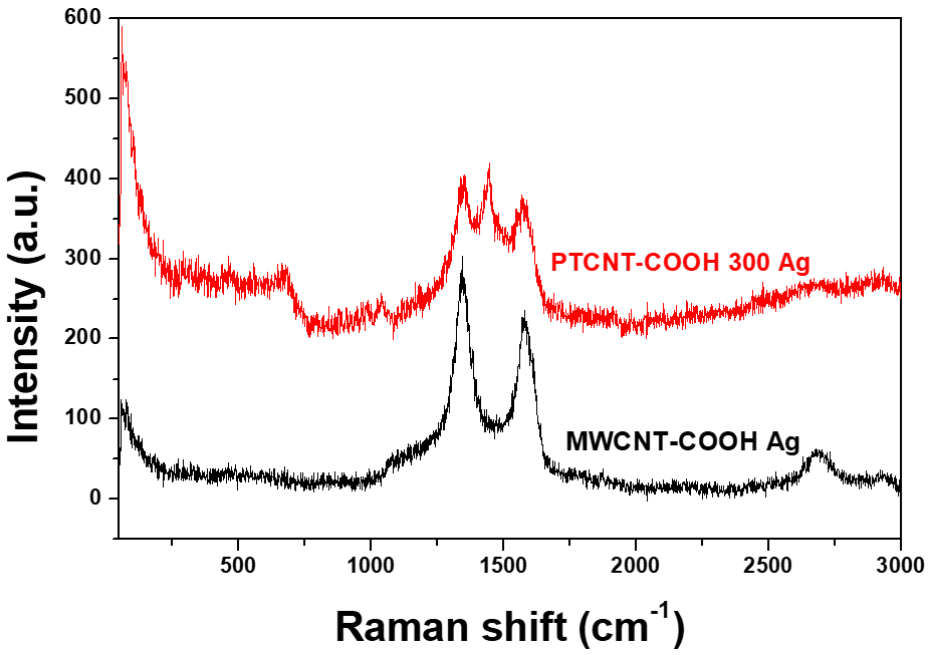

Figure 4.5. *FT Raman spectra of* ***MWCNT-COOH Ag*** *and* ***PTCNT-COOH 300 Ag***

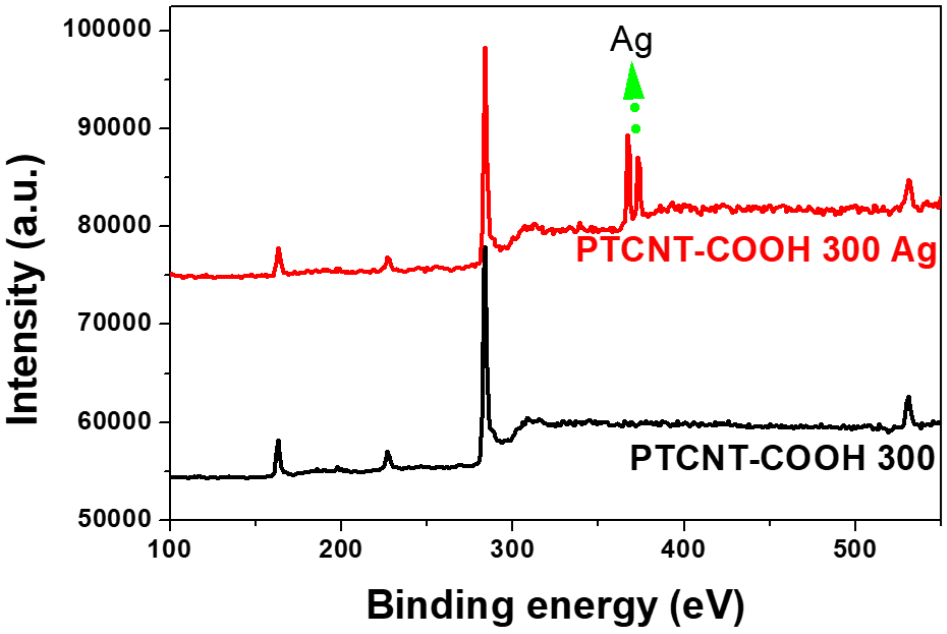

Figure 4.6. *XPS spectra of PTCNT-COOH 300 and PTCNT-COOH 300 Ag*

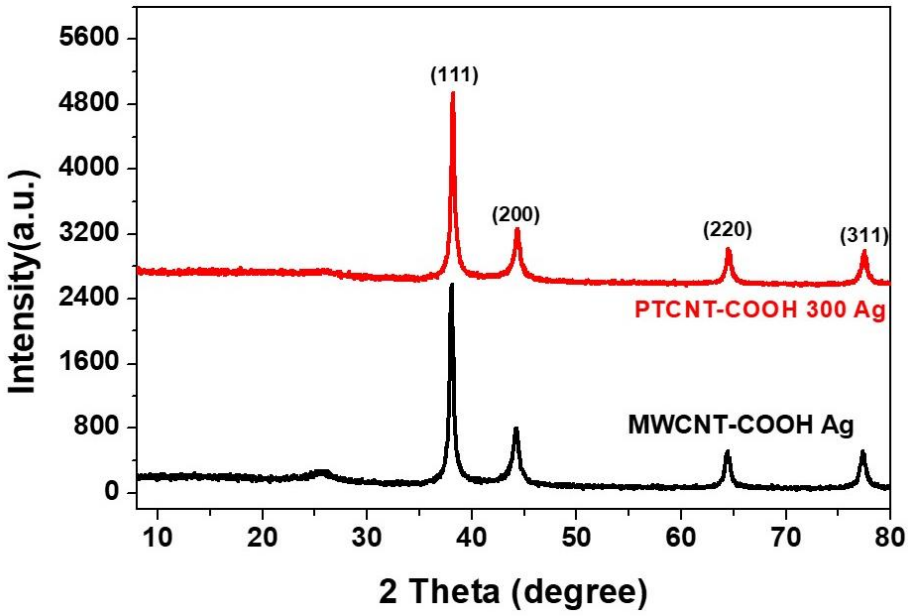

Figure 4.7. *WXRD pattern of PTCNT-COOH 300 Ag and MWCNT-COOH Ag*

The X-ray photoelectron spectra of PTCNT-COOH 300 and PTCNT-COOH 300 Ag have shown peaks at 162.75 eV, 226.95 eV, 283.25 eV and 531.45 eV corresponding to binding energies of S 2p, S 2s, C 1s and O 1s respectively. In addition, ternary silver nanocomposites PTCNT-COOH 300 Ag have shown peaks of silver atoms at 367.45 and 373.45 eV representing binding energies of $3d^{5/2}$ and $3d^{3/2}$ respectively, which indicates the formation of silver nanoparticles in the

nanocomposites (see **Figure 4.6.**).[34] Wide angle X-ray diffraction studies of PTCNT-COOH 300 Ag and MWCNT-COOH Ag have also been carried out to confirm the formation of silver nanoparticles in conducting polythiophene-functionalized MWCNT nanocomposites (see **Figure 4.7.**). Both the samples have shown highly crystalline peaks at 2θ values 38.15°, 44.33°, 64.52°and 77.46°, which represent Bragg's reflections from (111), (200), (220) and (311) planes of Ag nanoparticles in nanocomposites.[35] The weak peak at 2θ value 26.69° was due to diffraction from (002) plane of the graphitic structure of CNT.[36] The presence of highly crystalline silver nanoparticles increases the overall solid state ordering of the samples.

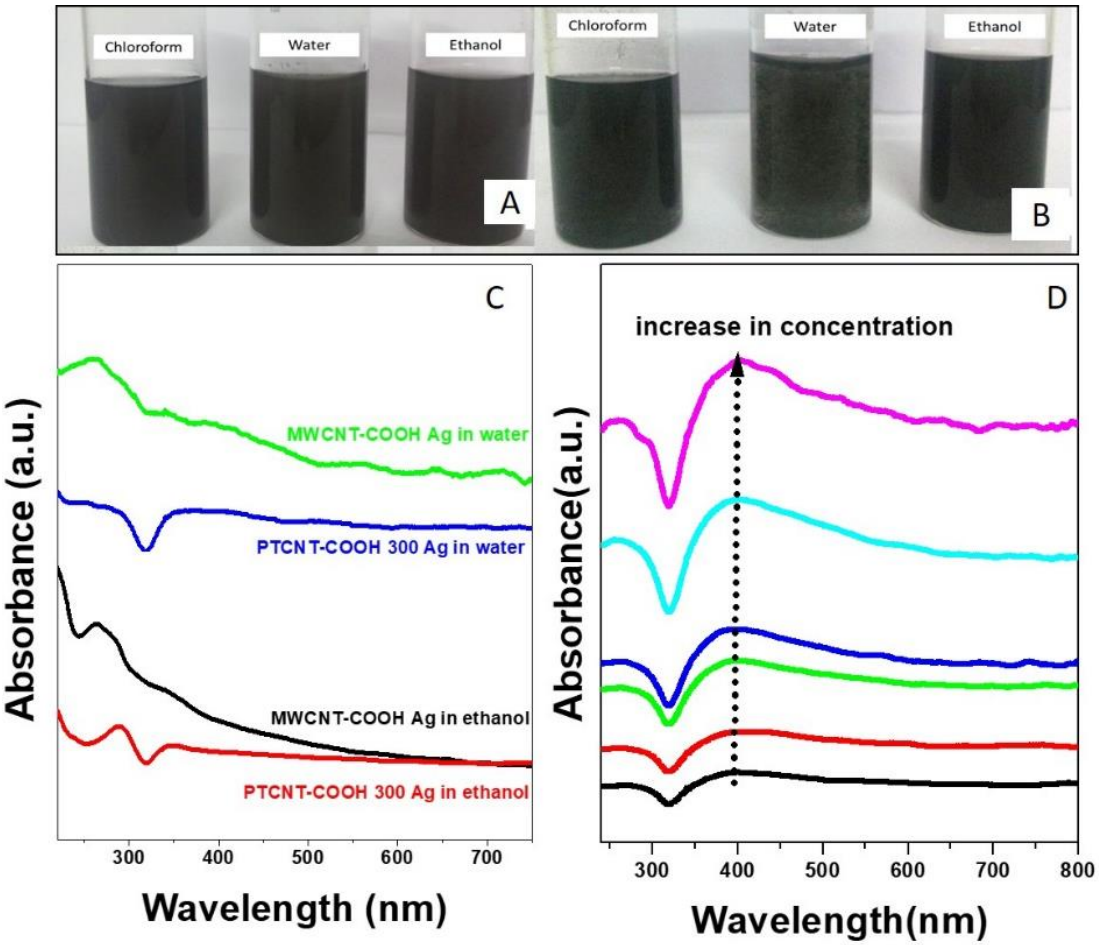

Figure 4.8. *Dispersion of PTCNT-COOH 300 Ag (A) and MWCNT-COOH Ag (B) in different solvents. UV-vis spectra of PTCNT-COOH 300 Ag and MWCNT-COOH Ag in water and ethanol (C). UV-vis spectra of PTCNT-COOH 300 Ag in water with different concentrations (D).*

MWCNT-COOH Ag and PTCNT-COOH 300 Ag could be easily dispersed in water and ethanol, allowing us to record the UV-vis absorption spectra (see **Figure**

4.8.). The tendency of formation of stable dispersions was retained in ternary composite by keeping an energy barrier against aggregation. Whereas, in the case of binary silver nanocomposite the dispersion get settled down after 30 min. The UV-vis absorption spectra have shown absorption maxima at 285 nm due to the π-π* absorption from multiwalled carbon nanotube. The ternary nanocomposites PTCNT-COOH 300 Ag samples in water and ethanol have shown polaron- π peak at 360 nm. Surprisingly, the longer wavelength peak at 360 nm was extended as shoulder up to 550 nm, which could be attributed to the surface plasmon resonance of silver nanoparticles.[37,38]

4.3.2. Morphological analysis of ternary and binary silver nanocomposites

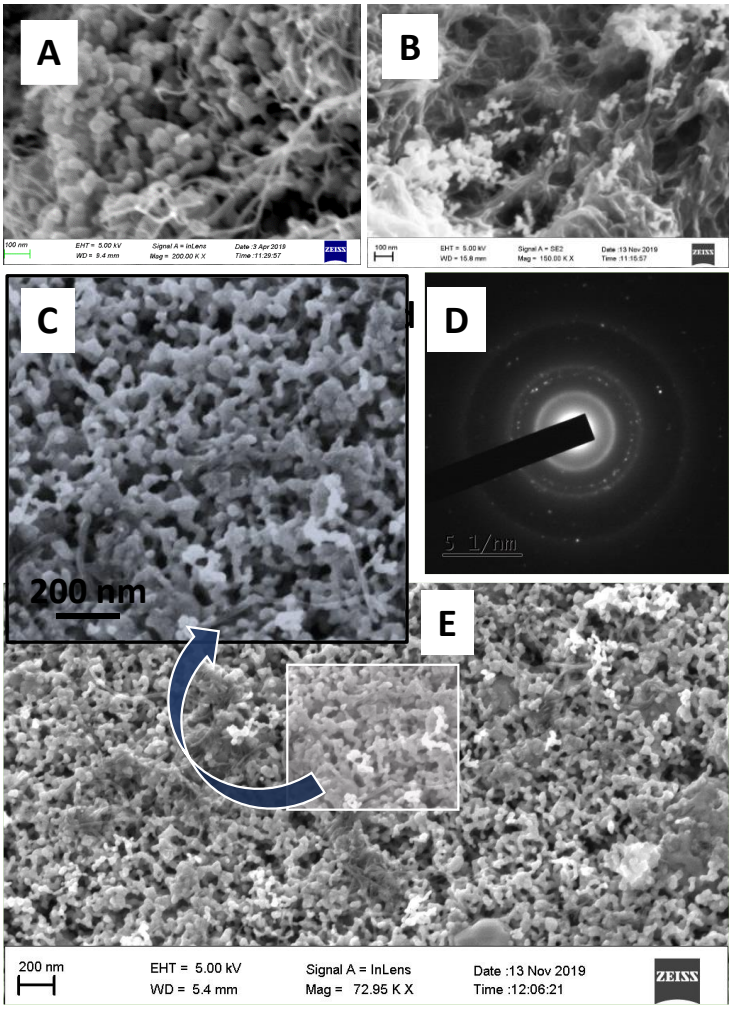

Figure 4.9. *FE-SEM images of MWCNT-COOH Ag (A), dispersed PTCNT-COOH 300 Ag (B), PTCNT-COOH 300 Ag (C (cropped image) and E) and electron diffraction pattern of PTCNT-COOH 300 Ag (D)*

The field emission scanning electron microscopic images of MWCNT-COOH Ag and PTCNT-COOH 300 Ag and dispersed PTCNT-COOH 300 Ag exhibited silver nanoparticles embedded the conducting polymer-carbon nanocomposites (see **Figure 4.9. (A),(B), (C)** and **(E)).** The striking observation made from field emission-scanning electron microscopy images of PTCNT-COOH 300 Ag was that embedded silver nanoparticles exhibited a tangled nature and spaces were observed between each nanotube of ternary nanocomposites. The predominant involvement of the non-covalent interaction of PTCNT-COOH 300 with silver nanoparticles (Ag) was evident from these images. Here nanocomposite were appeared without aggregation of silver atoms.

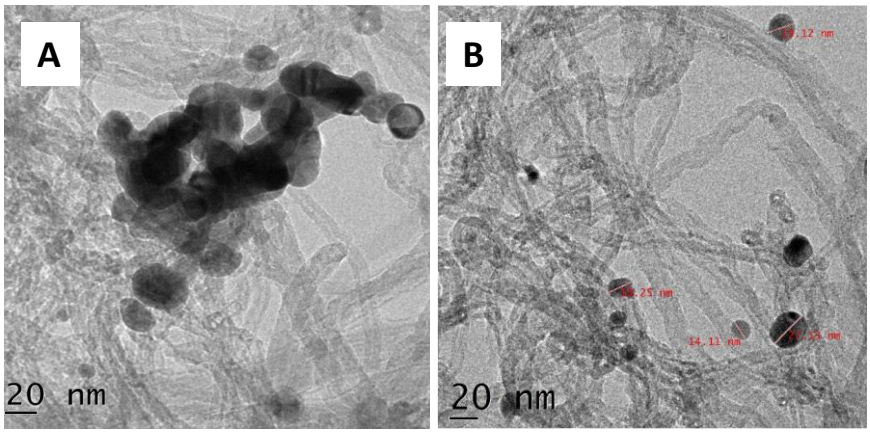

Figure 4.10. *Transmission electron microscopic images of PTCNT-COOH 300 Ag (A) and its size calculation (by taking the average size of 10 nanoparticles) (B)*

Transmission electron microscopic analysis of the nanoparticles has revealed the formation of tangled solid silver nanoparticles over PTCNT-COOH nanocomposites with an average size of 25 ± 5 nm obtained as an average of 10-12 nanoparticles (see **Figure 4.10.**). Entangled silver nanoparticles embedded over polythiophene-functionalized multiwalled carbon nanotube appear as aggregated silver particles. However, there were isolated nanoparticles in the PTCNT-COOH fibrous matrix and a close look at the silver nanoparticles revealed that they were embedded in the nanocomposite matrix. PTCNT-COOH 300 Ag has a ring-like electron diffraction pattern with bright spots, which indicates that Ag nanoparticles are crystalline (see **Figure 4.9. (D)**).[39]

It is important to note that silver nanoparticles have nearly spherical shapes even though they exist in tangled fashion, as seen in **Figure 4.11.** In the case of ternary silver nanocomposites formation, the Ag^{+} ions from silver nitrate were attracted to sulfur

atoms in the heterocyclic polythiophene chains and get reduced to silver nanoparticles by accepting electrons from ascorbic acid present in the aqueous dispersion. Ascorbic acid itself is converted to semidehydroascorbic acid radical ion and then to dehydroascorbic acid.[34,40] Anchoring of silver nanoparticles to the surface of the nanocomposites occurs via its complex formation with the sulfur atoms and the carboxylate group contained in PTCNT-COOH nanocomposites.[41,42] The sulfur atoms in closely packed polythiophene chains can assist the silver nanoparticles to decorate over the PTCNT-COOH 300 in a tangling fashion along with the carboxylic group of functionalized carbon nanotubes using the non-covalent force of interactions.

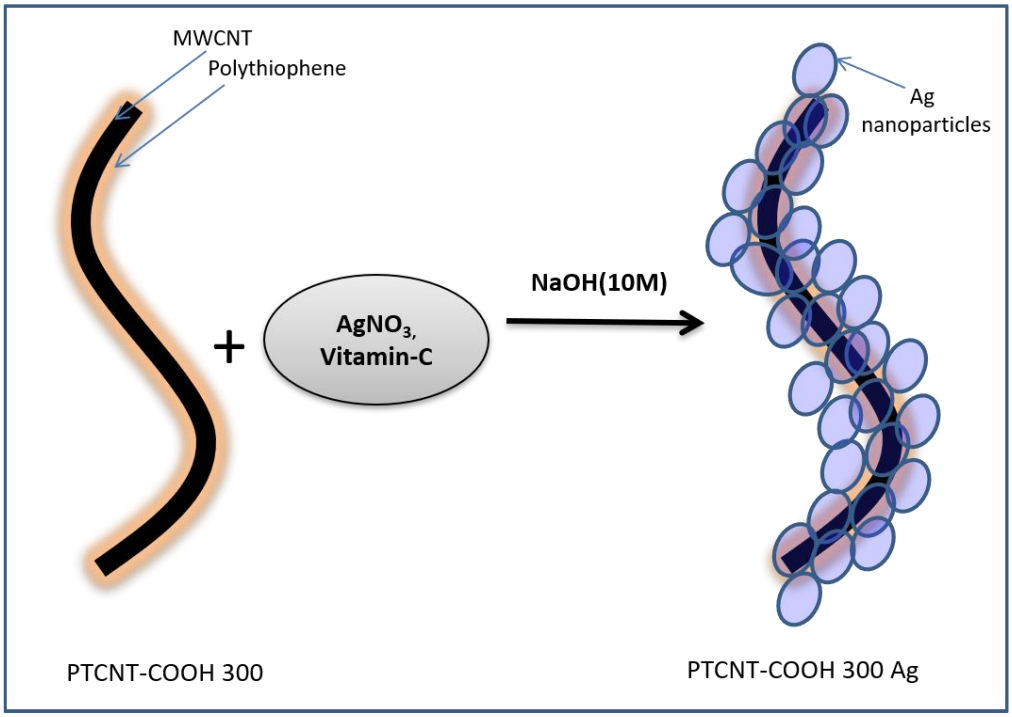

Figure 4.11. *Scheme for the formation of silver nanoparticle embedded ternary nano composite.*

4.3.3. Electrical conductivity and thermal stability of ternary and binary nanocomposites

The four-probe electrical conductivity of the samples was recorded by DFP-RM-200 four-probe set-up with a constant current. The electrical conductivity of the samples was measured at four different points and the average value has been reported. The electrical conductivity of the PTCNT-COOH 300, MWCNT, MWCNT-COOH Ag

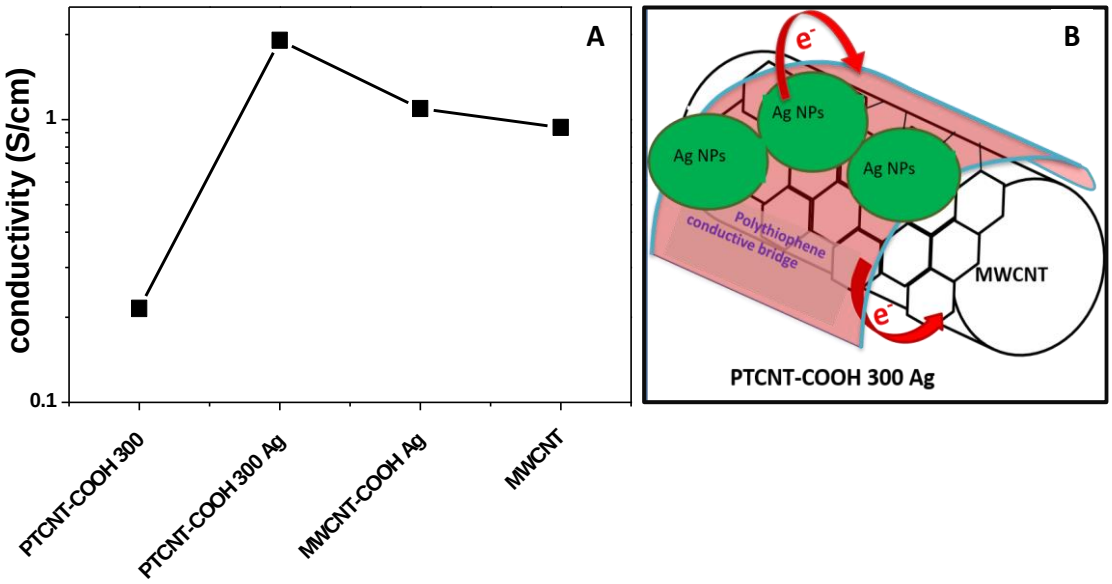

Figure 4.12. *Four probe electrical conductivity measurements of PTCNT- COOH 300, PTCNT-COOH 300 Ag and MWCNT-COOH Ag and pristine MWCNT (A). The schematic illustration of polythiophene as a connecting bridge between MWCNT-COOH and silver nanoparticles (B).*

and PTCNT-COOH 300 Ag were 1.64, 8.66, 12.40 and 80.76 S/cm, respectively (see **Figure 4.12. (a)**). The electrical conductivity of polythiophene was less than pristine multiwalled carbon nanotube and polythiophene-functionalized multiwalled carbon nanotube binary nanocomposites. Effective charge transfer of the charge carriers in binary and ternary nanocomposites resulted in higher electrical conductivity. The silver nanoparticles loaded polythiophene-functionalized MWCNT nanocomposites were an interesting case of ternary conducting polymer nanocomposite due to conducting polythiophene layer. The conducting polythiophene layer acts as a conductive bridge that transfers electrical charges between more conducting silver and multiwalled carbon nanotube via a hopping mechanism. Therefore the overall electrical conductivity of the system increases (see **Figure 4.12 (b)**).

Thermal stability of PTCNT-COOH 300, MWCNT-COOH Ag and PTCNT-COOH 300 Ag have been carried out using thermogravimetric analysis at a heating rate of 20°C per minute under an inert nitrogen atmosphere (see **Figure 4.13.**). The thermal stability of PTCNT-COOH 300 Ag was found to be higher than PTCNT-COOH 300. Sample PTCNT-COOH 300 Ag has shown 10 % weight loss at 620°C.[43]

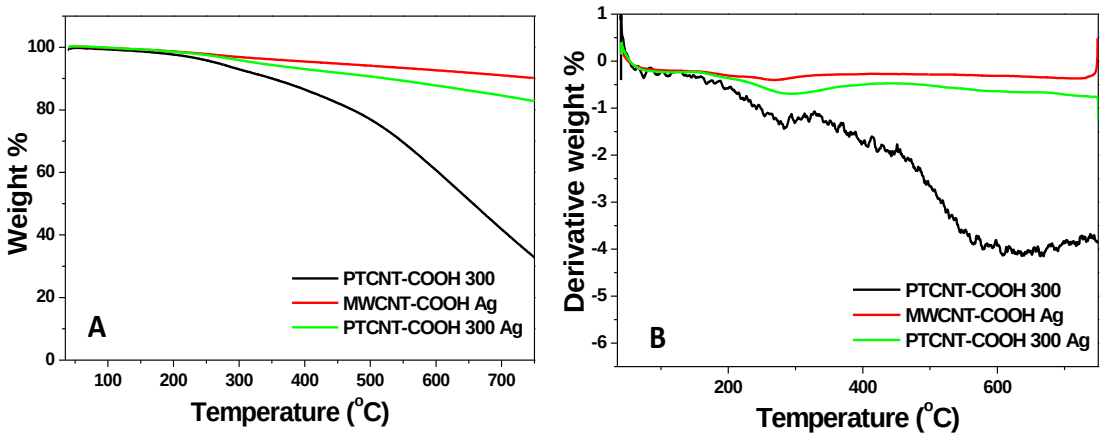

Figure 4.13. *Thermograms (A) and differential thermograms (B) of PTCNT-COOH 300, MWCNT-COOH Ag and PTCNT-COOH 300 Ag*

Accommodation of silver nanoparticles in ternary composite PTCNT-COOH 300 Ag enhances the thermal conductivity of the system.[44] The high thermal conductivity of multiwalled carbon nanotube and silver nanoparticles might have played a crucial role in enhancing thermal stability by building a perfect heat transfer network in ternary nanocomposites even though it contains a high percentage of thermally less stable polythiophene.[45] The highest thermal stability obtained for MWCNT-COOH Ag for 10% weight loss was 750 °C, which was devoid of the polymer sample. Therefore, the thermal stability and thermal conductivity of PTCNT-COOH 300 (binary composite) and functionalized MWCNT-COOH could be increased significantly by making entangled sliver nanoparticle ternary nanocomposites.[46] Differential thermal analysis exhibited that decomposition of functionalized MWCNT-COOH was observed from 510˚ C. Whereas decomposition rate of PTCNT-COOHs was observed in two stages, one stage from 260 to 340˚C due to degradation of polythiophene and the other one starting from 470˚C due to the CNT structural decomposition (see **Figure 4.13. (b)**). Good thermal stability of MWCNT-COOH Ag and PTCNT-COOH 300 Ag was observed with a much lower rate of decomposition, so they can perform as suitable materials in high temperature applications.

The pH sensitivity of the ternary nanocomposite system has been checked by the leaching tendency of embedded silver in ternary nanocomposite in acidic, basic and neutral media (see **Figure 4.14.**). The stability of the ternary nanocomposites at

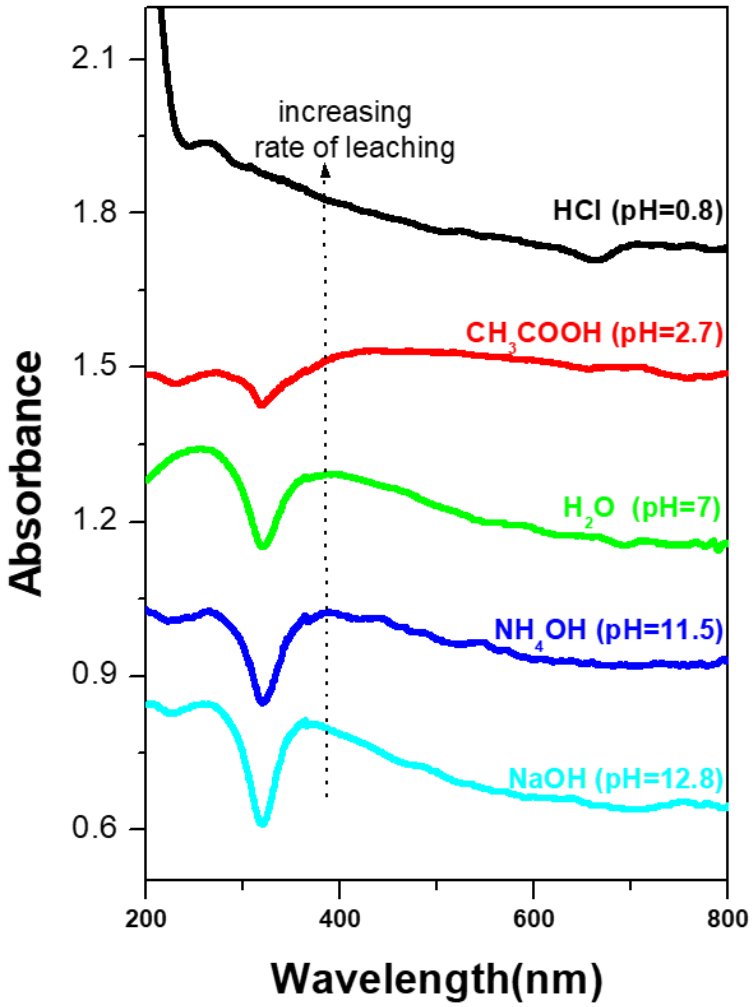

Figure 4.14. *UV-vis spectra of PTCNT-COOH 300 Ag after 3 h of stirring and washing with different media of different pH.*

different pH has been checked via UV-vis absorption spectroscopy by noting the changes in the surface plasmon peak (> 360 nm). The study revealed that silver nanoparticles have good stability against leaching in basic medium (high pH). Compared to NaOH medium, leached silver nanoparticles percentage in other media such as NH_4OH, H_2O and CH_3COOH are 11.79%, 29.23% and 60% respectively. Badawy et al. reported that electrostatically stabilized silver nanoparticles exhibit high degree of aggregation at low pH (acidic conditions). The surface charge densities will be less negative at low pH of the medium and resulted higher particle-particle interaction. As pH of the medium decreases the silver nanoparticles get aggregated easily and into larger particles. The larger particles get leached out easily from the surface of composite.[47] Ternary nanocomposites can be effectively utilized for catalytic applications in a basic medium and therefore, they can be a durable catalyst with

***Table 4.2**. Comparison study of our work with similar systems reported in the literature.*

	components	Synthetic method of nanoparticles	Solvent/solvents used for synthesis of nanoparticles	Reducing agent/reagent for nanoparticle synthesis	Size of nanoparticles	Functionalizations carried out for MWCNT	Suggesting dispersion medium for further processing	Conductivity S/cm	Thermal stability	Extended study based on application	Reference number
Our work	Polythiophene, acid functionalized MWCNT, silver nanoparticles	Chemical	H_2O	Vitamin-C-reductant	25±8 nm	Carboxylic acid functionalization	H_2O, ethanol	80.76 S/cm	10% weight loss at ~620°	Leaching study of silver nanoparticles in different pH	_
Same system in literature	PEDOT/polystyrene sulfonate, MWCNT, silver nanoparticles	Chemical	DCM	$NaBH_4$-reductant	~128± 28 nm	Ethylene diamine functionalization	DCM	_	_	Improving electrical conductivity of polycarbonate matrix	15
Similar Systems in literature	Poly(2-thiophene methyl amine), MWCNT, CdS nanoparticles	Chemical	DMF and water	Na_2S-reagent	Average size=3.1 nm	_	_	_	10% weight loss at ~320°	Optical limiting enhancement	48
	Polythiophene, MWCNT, gold nanoparticles	Chemical	H_2O	Thiophene-reductant	average size=4.3 nm	_	_	_	_	_	41
	Polythiophene, MWCNT, gold nanoparticles	Chemical	Hexane and H_2O	Thiophene-reductant	~5 nm and ~15 nm	_	_	_	_	Electrochemical sensing of dopamine	50
	Polythiophene, MWCNT, platinum nanoparticles	Electrochemical	_	_	Nanocluster formation -	Oxidation by acid treatment	_	_	_	Electrochemical sensor for Bisphenol A	51
	Polyaniline, MWCNT, silver nanoparticles	Chemical	H_2O	Aniline	Single nanoparticles - 5-30 nm Agglomerated nanoparticles - 50-95 nm	Carboxylic acid functionalization	_	4.24 S/cm	10% weight loss at ~320°	High performance supercapacitor electrode	2
	Polypyrrole, MWCNT, silver nanoparticles	Chemical	H_2O	Trisodium citrate dihydrate	30 nm	Carboxylic acid functionalization	_	4.01 S/cm	_	Electromagnetic shielding	49
		UV-reduction	H_2O	UV	30-35 nm	Carboxylic acid functionalization	_	5.12 S/cm			

multiple uses.[48,49] Present work has significant advantages over other systems, especially in cost, efficiency and many other improved properties related to conductivity and thermal stability in nanocomposites. Synthesis of tangled silver nanoparticles embedded on polythiophene-functionalized multiwalled carbon nanotubes have been adopted in the cheapest and greener medium. Comparison of ternary and binary silver nanocomposites with other literatures are given in **Table 4.2.** The binary and ternary nanocomposites have been prepared efficiently on a laboratory scale with reproducibility and with improved processability. Therefore, the ternary nanocomposites prepared will open a doorway to different applications such as high-performance electrochemical electrodes, polymer supercapacitors, sensors, SERS tags, thermoelectric materials, catalytic applications and so on.[49-53]

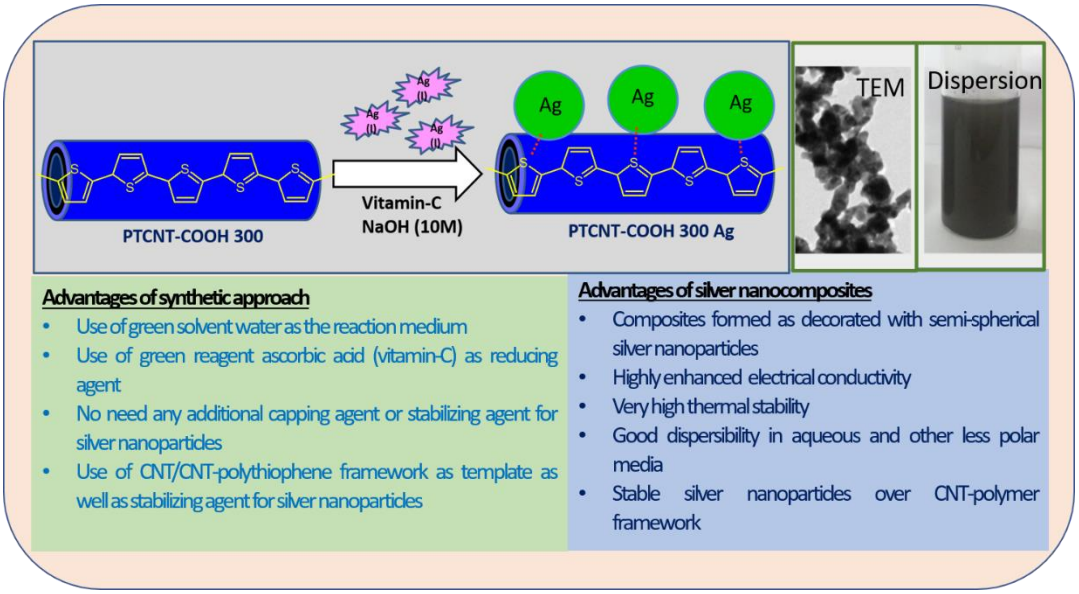

Figure 4.15. *Illustration of the formation of water-dispersible ternary nanocomposite and its advantageous outcomes.*

4.4. Conclusion

In summary, the present work demonstrated a facile and green synthetic approach to prepare water-dispersible, highly conductive and thermally stable ternary silver nanoparticles embedded polythiophene-functionalized multiwalled carbon nanotube nanocomposite (PTCNT-COOH 300 Ag) by efficiently utilizing the aqueous dispersion of binary polythiophene-functionalized multiwalled carbon nanotube nanocomposites (PTCNT-COOH 300) as a nanofibrous platform as well as the co-component matrix in its ternary composite. Here, we could effectively establish a facile synthesis of PTCNT-COOH 300 Ag from the dispersed state of PTCNT-COOH 300

binary composite by reduction of silver nitrate using ascorbic acid in green solvent water. A binary multiwalled carbon nanotube-silver nanocomposites (MWCNT-COOH Ag) were also synthesised using a similar in-situ reduction strategy. Formation of PTCNT-COOH 300 Ag and MWCNT-COOH Ag were primarily characterized by FT-IR spectroscopy, FT-Raman spectroscopy, XPS analysis and X-ray diffraction pattern analysis. The formation of crystalline silver nanoparticles in PTCNT-COOH 300 Ag was confirmed by WXRD analysis by noting the sharp crystalline peaks at 38.15°, 44.33°, 64.52°and 77.46° indicated by Bragg's reflections from (111), (200), (220) and (311) planes. Scanning and transmission electron microscopic analysis gave information about the formation of embedded silver nanoparticles on PTCNT-COOH 300 with an average size of 25 ± 8 nm in PTCNT-COOH 300 Ag. UV-vis spectra of PTCNT-COOH 300 Ag and MWCNT-COOH Ag have shown surface plasmon resonance of silver nanoparticles as a shoulder up to 550 nm. Tangled silver nanoparticles formed in the ternary nanocomposites were embedded over polythiophene-functionalized multiwalled carbon nanotube by the complex formation of sulfur atoms of thiophene moiety with silver. PTCNT-COOH 300 Ag exhibited higher electrical conductivity and thermal stability (two times higher) than PTCNT-COOH 300 for 10% weight loss due to the presence of embedded silver nanoparticles. The important and promising outcomes of the present investigations were summarized in **Figure 4.15**. The silver nanocomposites could effectively utilize catalytical, antibacterial, electrical and thermal applications based on their dispersibility, reusability, enhanced electrical conductivity and thermal stability.

References

1. Watt, J.; Collins, A. M.; Vreeland, E. C.; Montano, G. A.; Huber, D. L. Magnetic Nanocomposites and Their Incorporation into Higher Order Biosynthetic Functional Architectures. *ACS Omega* **2018**, *3* (1), 503–508. https://doi.org/10.1021/acsomega.7b02031.
2. Dhibar, S.; Das, C. K. Silver Nanoparticles Decorated Polyaniline/Multiwalled Carbon Nanotubes Nanocomposite for High-Performance Supercapacitor Electrode. *Ind. Eng. Chem. Res.* **2014**, *53* (9), 3495–3508. https://doi.org/10.1021/ie402161e.
3. Feng, M.; Sun, R.; Zhan, H.; Chen, Y. Decoration of Carbon Nanotubes with CdS Nanoparticles by Polythiophene Interlinking for Optical Limiting Enhancement. *Carbon N. Y.* **2010**, *48* (4), 1177–1185. https://doi.org/10.1016/j.carbon.2009.11.041.
4. Ohlan, A.; Singh, K.; Chandra, A.; Dhawan, S. K. Microwave Absorption Behavior of Core?Shell Structured Poly (3,4-Ethylenedioxy Thiophene)?Barium Ferrite Nanocomposites. *ACS Appl. Mater. Interfaces* **2010**, *2* (3), 927–933. https://doi.org/10.1021/am900893d.

5. Chakraborty, I.; Chakrabarty, N.; Senapati, A.; Chakraborty, A. K. CuO@NiO/Polyaniline/MWCNT Nanocomposite as High-Performance Electrode for Supercapacitor. *J. Phys. Chem. C* **2018**, *122* (48), 27180–27190. https://doi.org/10.1021/acs.jpcc.8b08091.
6. Malekkiani, M.; Heshmati Jannat Magham, A.; Ravari, F.; Dadmehr, M. Facile Fabrication of Ternary MWCNTs/ZnO/Chitosan Nanocomposite for Enhanced Photocatalytic Degradation of Methylene Blue and Antibacterial Activity. *Sci. Rep.* **2022**, *12* (1). https://doi.org/10.1038/s41598-022-09571-5.
7. Hou, Y.; Cheng, Y.; Hobson, T.; Liu, J. Design and Synthesis of Hierarchical MnO2 Nanospheres/Carbon Nanotubes/Conducting Polymer Ternary Composite for High Performance Electrochemical Electrodes. *Nano Lett.* **2010**, *10* (7), 2727–2733. https://doi.org/10.1021/nl101723g.
8. Tang, L.; Duan, F.; Chen, M. Silver Nanoparticle Decorated Polyaniline/Multiwalled Super-Short Carbon Nanotube Nanocomposites for Supercapacitor Applications. *RSC Adv.* **2016**, *6* (69), 65012–65019. https://doi.org/10.1039/c6ra12442a.
9. Patole, A.; Ventura, I. A.; Lubineau, G. Thermal Conductivity and Stability of a Three-Phase Blend of Carbon Nanotubes, Conductive Polymer, and Silver Nanoparticles Incorporated into Polycarbonate Nanocomposites. *J. Appl. Polym. Sci.* **2015**, *132* (30). https://doi.org/10.1002/app.42281.
10. Drury, A.; Chaure, S.; Kröll, M.; Nicolosi, V.; Chaure, N.; Blau, W. J. Fabrication and Characterization of Silver/Polyaniline Composite Nanowires in Porous Anodic Alumina. *Chem. Mater.* **2007**, *19* (17), 4252–4258. https://doi.org/10.1021/cm071102s.
11. Abou El-Nour, K. M. M.; Eftaiha, A.; Al-Warthan, A.; Ammar, R. A. A. Synthesis and Applications of Silver Nanoparticles. *Arab. J. Chem.* **2010**, *3* (3), 135–140. https://doi.org/10.1016/j.arabjc.2010.04.008.
12. Dhibar, S.; Das, C. K. Silver Nanoparticles Decorated Polyaniline/Multiwalled Carbon Nanotubes Nanocomposite for High-Performance Supercapacitor Electrode. *Ind. Eng. Chem. Res.* **2014**, *53* (9), 3495–3508. https://doi.org/10.1021/ie402161e.
13. Tang, L.; Duan, F.; Chen, M. Silver Nanoparticle Decorated Polyaniline/Multiwalled Super-Short Carbon Nanotube Nanocomposites for Supercapacitor Applications. *RSC Adv.* **2016**, *6* (69), 65012–65019. https://doi.org/10.1039/c6ra12442a.
14. Sarkar. A. K.; Sahna. A.;Banerjee. C.; Mandre. N. R.; Panda. A. B.; Pal. S. Crosslinked Biopolymer Stabilized Exfoliated Titanate Nano Sheet Supported AgNPs: A Green Sustainable Ternary Nanocomposite Hydrogel for Catalytic and Antimicrobial Activity, Sustainable Chem. Eng. 2017, 5 (2), 1881-1891. https://doi.org/10.1021/acssuschemeng.6b02594.
15. Patole, A.; Lubineau, G. Carbon Nanotubes with Silver Nanoparticle Decoration and Conductive Polymer Coating for Improving the Electrical Conductivity of Polycarbonate Composites. *Carbon N. Y.* **2015**, *81* (1), 720–730. https://doi.org/10.1016/j.carbon.2014.10.014.
16. Reddy, K. R.; Sin, B. C.; Ryu, K. S.; Kim, J. C.; Chung, H.; Lee, Y. Conducting Polymer Functionalized Multi-Walled Carbon Nanotubes with Noble Metal Nanoparticles: Synthesis, Morphological Characteristics and Electrical Properties. *Synth. Met.* **2009**, *159* (7–8), 595–603. https://doi.org/10.1016/j.synthmet.2008.11.030.
17. Elhalawany, N.; Awad, M. A.; Zahran, M. K. Synthesis, Characterization, Optical and Electrical Properties of Novel Highly Dendritic Polythiophene Nanocomposites with Silver and/or Gold. *J. Mater. Sci. Mater. Electron.* **2018**, *29* (11), 8970–8977. https://doi.org/10.1007/s10854-018-8921-7.
18. Lee, C. J.; Karim, M. R.; Lee, M. S. Synthesis and Characterization of Silver/Thiophene Nanocomposites by UV-Irradiation Method. *Mater. Lett.* **2007**, *61* (13), 2675–2678. https://doi.org/10.1016/j.matlet.2006.10.021.
19. Ates, M.; Caliskan, S.; Ozten, E. A Ternary Nanocomposite of Reduced Graphene Oxide, Ag Nanoparticle and Polythiophene Used for Supercapacitors. *Fullerenes Nanotub. Carbon Nanostructures* **2018**, *26* (6), 360–369. https://doi.org/10.1080/1536383X.2018.1438414.

20. Tessonnier, J. P.; Ersen, O.; Weinberg, G.; Pham-Huu, C.; Su, D. S.; Schlögl, R. Selective Deposition of Metal Nanoparticles inside or Outside Multiwalled Carbon Nanotubes. *ACS Nano* **2009**, *3* (8), 2081–2089. https://doi.org/10.1021/nn900647q.
21. Shaham, G.; Veisi, H.; Hekmati, M. Silver Nanoparticle-Decorated Multiwalled Carbon Nanotube/Pramipexole Nanocomposite: Synthesis, Characterization and Application as an Antibacterial Agent. *Appl. Organomet. Chem.* **2017**, *31* (10). https://doi.org/10.1002/aoc.3737.
22. Tran Hoang, P.; Salazar, N.; Porkka, T. N.; Joshi, K.; Liu, T.; Dickens, T. J.; Yu, Z. Engineering Crack Formation in Carbon Nanotube-Silver Nanoparticle Composite Films for Sensitive and Durable Piezoresistive Sensors. *Nanoscale Res. Lett.* **2016**, *11* (1). https://doi.org/10.1186/s11671-016-1626-z.
23. Lee, J. W.; Cho, J. Y.; Kim, M. J.; Kim, J. H.; Park, J. H.; Jeong, S. Y.; Seo, S. H.; Lee, G. W.; Jeong, H. J.; Han, J. T. Synthesis of Silver Nanoparticles Embedded with Single-Walled Carbon Nanotubes for Printable Elastic Electrodes and Sensors with High Stability. *Sci. Rep.* **2021**, *11* (1). https://doi.org/10.1038/s41598-021-84386-4.
24. Castle, A. B.; Gracia-Espino, E.; Nieto-Delgado, C.; Terrones, H.; Terrones, M.; Hussain, S. Hydroxyl-Functionalized and N-Doped Multiwalled Carbon Nanotubes Decorated with Silver Nanoparticles Preserve Cellular Function. *ACS Nano* **2011**, *5* (4), 2458–2466. https://doi.org/10.1021/nn200178c.
25. Olivares, F.; Peón, F.; Henríquez, R.; del Río, R. S. Strategies for Area-Selective Deposition of Metal Nanoparticles on Carbon Nanotubes and Their Applications: A Review. *J. Mater. Sci.* **2022**, *57* (4), 2362–2387. https://doi.org/10.1007/s10853-021-06710-7.
26. Zhang, S.; Lu, Q.; Zhang, C.; Zhou, Y.; Liu, M.; Zhang, Y.; Deng, L. Green Synthesis of Silver-Carbon Nanocomposites with Extraordinary Stability and Robust Antibacterial Activity against Bacterial Diseases in Fish. *ACS Appl. Bio Mater.* **2022**, *5* (3), 1064–1072. https://doi.org/10.1021/acsabm.1c01116.
27. Kumari, S.; Sharma, P.; Yadav, S.; Kumar, J.; Vij, A.; Rawat, P.; Kumar, S.; Sinha, C.; Bhattacharya, J.; Srivastava, C. M.; Majumder, S. A Novel Synthesis of the Graphene Oxide-Silver (GO-Ag) Nanocomposite for Unique Physiochemical Applications. *ACS Omega* **2020**, *5* (10), 5041–5047. https://doi.org/10.1021/acsomega.9b03976.
28. AL-Refai, H. H.; Ganash, A. A.; Hussein, M. A. Polythiophene and Its Derivatives –Based Nanocomposites in Electrochemical Sensing: A Mini Review. *Mater. Today Commun.* **2021**, *26*. https://doi.org/10.1016/j.mtcomm.2020.101935.
29. Tang, L.; Duan, F.; Chen, M. Silver Nanoparticle Decorated Polyaniline/Multiwalled Super-Short Carbon Nanotube Nanocomposites for Supercapacitor Applications. *RSC Adv.* **2016**, *6* (69), 65012–65019. https://doi.org/10.1039/c6ra12442a.
30. Wilson, J.; Radhakrishnan, S.; Sumathi, C.; Dharuman, V. Polypyrrole-Polyaniline-Au (PPy-PANi-Au) Nano Composite Films for Label-Free Electrochemical DNA Sensing. *Sensors Actuators, B Chem.* **2012**, *171–172*, 216–222. https://doi.org/10.1016/j.snb.2012.03.019.
31. Miller, A. J.; Hatton, R. A.; Silva, S. R. P. Water-Soluble Multiwall-Carbon-Nanotube-Polythiophene Composite for Bilayer Photovoltaics. *Appl. Phys. Lett.* **2006**, *89* (12). https://doi.org/10.1063/1.2356115.32.
32. Bazzaoui, E. A.; Lévi, G.; Aeiyach, S.; Aubard, J.; Marsault, J. P.; Lacaze, P. C. SERS Spectra of Polythiophene in Doped and Undoped States. *J. Phys. Chem.* **1995**, *99* (17), 6628–6634. https://doi.org/10.1021/j100017a052.
33. Shi, G.; Xu, J.; Fu, M. Raman Spectroscopic and Electrochemical Studies on the Doping Level Changes of Polythiophene Films during Their Electrochemical Growth Processes. *J. Phys. Chem. B* **2002**, *106* (2), 288–292. https://doi.org/10.1021/jp013023o.
34. Zhang, N.; Yu, X.; Hu, J.; Xue, F.; Ding, E. Synthesis of Silver Nanoparticle-Coated Poly(Styrene-Co-Sulfonic Acid) Hybrid Materials and Their Application in Surface-

Enhanced Raman Scattering (SERS) Tags. *RSC Adv.* **2013**, *3* (33), 13740–13747. https://doi.org/10.1039/c3ra40888d.
35. Jiang, H.; Moon, K. S.; Li, Y.; Wong, C. P. Surface Functionalized Silver Nanoparticles for Ultrahigh Conductive Polymer Composites. *Chem. Mater.* **2006**, *18* (13), 2969–2973. https://doi.org/10.1021/cm0527773.36.
36. Li, H.; Zhou, B.; Lin, Y.; Gu, L.; Wang, W.; Fernando, K. A. S.; Kumar, S.; Allard, L. F.; Sun, Y. P. Selective Interactions of Porphyrins with Semiconducting Single-Walled Carbon Nanotubes. *J. Am. Chem. Soc.* **2004**, *126* (4), 1014–1015. https://doi.org/10.1021/ja037142o.
37. Ranjan, P.; Shankar, S.; Popovitz-Biro, R.; Cohen, S. R.; Kaplan-Ashiri, I.; Dadosh, T.; Shimon, L. J. W.; Višić, B.; Tenne, R.; Lahav, M.; Van Der Boom, M. E. Decoration of Inorganic Nanostructures by Metallic Nanoparticles to Induce Fluorescence, Enhance Solubility, and Tune Band Gap. *J. Phys. Chem. C* **2018**, *122* (12), 6748–6759. https://doi.org/10.1021/acs.jpcc.8b00510.
38. Lee, C. J.; Karim, M. R.; Lee, M. S. Synthesis and Characterization of Silver/Thiophene Nanocomposites by UV-Irradiation Method. *Mater. Lett.* **2007**, *61* (13), 2675–2678. https://doi.org/10.1016/j.matlet.2006.10.021.
39. Dhibar, S.; Das, C. K. Electrochemical Performances of Silver Nanoparticles Decorated Polyaniline/Graphene Nanocomposite in Different Electrolytes. *J. Alloys Compd.* **2015**, *653*, 486–497. https://doi.org/10.1016/j.jallcom.2015.08.158.
40. Malassis, L.; Dreyfus, R.; Murphy, R. J.; Hough, L. A.; Donnio, B.; Murray, C. B. One-Step Green Synthesis of Gold and Silver Nanoparticles with Ascorbic Acid and Their Versatile Surface Post-Functionalization. *RSC Adv.* **2016**, *6* (39), 33092–33100. https://doi.org/10.1039/c6ra00194g.
41. Oliveira, M. M.; Zarbin, A. J. G. Carbon Nanotubes Decorated with Both Gold Nanoparticles and Polythiophene. *J. Phys. Chem. C* **2008**, *112* (48), 18783–18786. https://doi.org/10.1021/jp8052482.
42. Lee, C. J.; Karim, M. R.; Lee, M. S. Synthesis and Characterization of Silver/Thiophene Nanocomposites by UV-Irradiation Method. *Mater. Lett.* **2007**, *61* (13), 2675–2678. https://doi.org/10.1016/j.matlet.2006.10.021.
43. Kuila, B. K.; Park, K.; Dai, L. Soluble P3HT-Grafted Carbon Nanotubes: Synthesis and Photovoltaic Application. *Macromolecules* **2010**, *43* (16), 6699–6705. https://doi.org/10.1021/ma100917p.
44. Tamboli, M. S.; Kulkarni, M. V.; Patil, R. H.; Gade, W. N.; Navale, S. C.; Kale, B. B. Nanowires of Silver-Polyaniline Nanocomposite Synthesized via in Situ Polymerization and Its Novel Functionality as an Antibacterial Agent. *Colloids Surfaces B Biointerfaces* **2012**, *92*, 35–41. https://doi.org/10.1016/j.colsurfb.2011.11.006.
45. Zhan, Y.; Ren, Y.; Wan, X.; Zhang, J.; Zhang, S. Dielectric Thermally Conductive and Stable Poly(Arylene Ether Nitrile) Composites Filled with Silver Nanoparticles Decorated Hexagonal Boron Nitride. *Ceram. Int.* **2018**, *44* (2), 2021–2029. https://doi.org/10.1016/j.ceramint.2017.10.147.46.
46. M.T. Ramesan, V. Santhi, In situ synthesis, characterization, conductivity studies of polypyrrole/silver doped zinc oxide nanocomposites and their application for ammonia gas sensing, J. Mater. Sci. Mater. Electron. 28 (2017) 18804–18814. doi:10.1007/s10854-017-7830-5.
47. M.T. Ramesan, V. Santhi, In situ synthesis, characterization, conductivity studies of polypyrrole/silver doped zinc oxide nanocomposites and their application for ammonia gas sensing, J. Mater. Sci. Mater. Electron. 28 (2017) 18804–18814. doi:10.1007/s10854-017-7830-5.
48. El Badawy AM, Luxton TP, Silva RG, Scheckel KG, Suidan MT, Tolaymat TM. Impact of environmental conditions (pH, ionic strength, and electrolyte type) on the surface charge and aggregation of silver nanoparticles suspensions. Environ Sci Technol. 2010;44(4):1260–6.
49. Hedberg, J.; Skoglund, S.; Karlsson, M. E.; Wold, S.; Odnevall Wallinder, I.; Hedberg, Y. Sequential Studies of Silver Released from Silver Nanoparticles in Aqueous Media

Simulating Sweat, Laundry Detergent Solutions and Surface Water. *Environ. Sci. Technol.* **2014**, *48* (13), 7314–7322. https://doi.org/10.1021/es500234y.

50. No Title. https://doi.org/10.1021/es9035557.49. M. Feng, R. Sun, H. Zhan, Y. Chen, Decoration of carbon nanotubes with CdS nanoparticles by polythiophene interlinking for optical limiting enhancement, Carbon N. Y. 48 (2010) 1177–1185. doi:10.1016/j.carbon.2009.11.041.
51. I.Ebrahimi, M.P. Gashti, Polypyrrole-MWCNT-Ag composites for electromagnetic shielding: Comparison between chemical deposition and UV-reduction approaches, J. Phys. Chem. Solids. 118 (2018) 80–87. doi:10.1016/j.jpcs.2018.03.008.
52. Inagaki, C. S.; Oliveira, M. M.; Bergamini, M. F.; Marcolino-Junior, L. H.; Zarbin, A. J. G. Facile Synthesis and Dopamine Sensing Application of Three Component Nanocomposite Thin Films Based on Polythiophene, Gold Nanoparticles and Carbon Nanotubes. *J. Electroanal. Chem.* **2019**, *840*, 208–217. https://doi.org/10.1016/j.jelechem.2019.03.066.
53. Wan, J.; Si, Y.; Li, C.; Zhang, K. Bisphenol a Electrochemical Sensor Based on Multi-Walled Carbon Nanotubes/Polythiophene/Pt Nanocomposites Modified Electrode. *Anal. Methods* **2016**, *8* (16), 3333–3338. https://doi.org/10.1039/c6ay00850j.
54. Ebrahimi, I.; Gashti, M. P. Polypyrrole-MWCNT-Ag Composites for Electromagnetic Shielding: Comparison between Chemical Deposition and UV-Reduction Approaches. *J. Phys. Chem. Solids* **2018**, *118*, 80–87. https://doi.org/10.1016/j.jpcs.2018.03.008.